BIOCHEMISTRY
including biophysical chemistry & molecular biology

ARTICLE

pubs.acs.org/biochemistry

Normal Modes of Prion Proteins: From Native to Infectious Particle

Abraham O. Samson*,†,‡ and Michael Levitt†

†Department of Structural Biology, Stanford University, Stanford, California 94305, United States

‡Faculty of Medicine, Bar-Ilan University, Safed, Israel

Supporting Information

ABSTRACT: Prion proteins (PrP) are the infectious agent in transmissible spongiform encephalopathies (i.e., mad cow disease). To be infectious, prion proteins must undergo a conformational change involving a decrease in α-helical content along with an increase in β-strand content. This conformational change was evaluated by means of elastic normal modes. Elastic normal modes show a diminution of two α-helices by one and two residues, as well as an extension of two β-strands by three residues each, which could instigate the conformational change. The conformational change occurs in a region that is compatible with immunological studies, and it is observed more frequently in mutant prions that are prone to conversion than in wild-type prions because of differences in their starting structures, which are amplified through normal modes. These findings are valuable for our comprehension of the conversion mechanism associated with the conformational change in prion proteins.

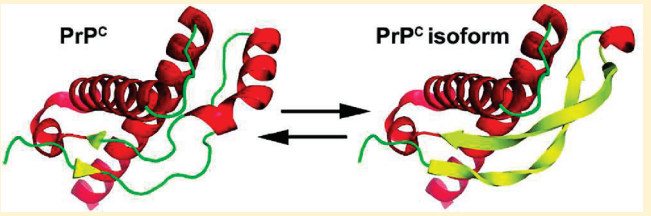

Prion proteins are the proteinaceous infectious particles in neurodegenerative transmissible spongiform encephalopathies (TSE or prion diseases).[1,2] Conversion of cellular PrP (PrP^C) into scrapie PrP (PrP^{SC}) and aggregation into cytotoxic oligomers are associated with a loss of neuronal cells, resulting in brain spongiosis, which in humans leads to debilitating, dementing, and invariably fatal diseases. Examples of TSEs include scrapies in ovines, "mad cow disease" in bovines, and Kuru, Creutzfeld-Jacob disease (CJD), fatal familial insomnia (FFI), and Gerstmann-Straussler-Scheinker syndrome (GSS) in humans.[3,4]

The prion protein in its native state (PrP^C) is a cell surface receptor anchored to the membrane by a glycosylphosphatidylinositol (GPI) at position S230 and carrying two glycosylation sites at N181 and N197 (numbering follows the human species). The PrP^C structure is composed of three helices, namely, H1 (residues 144−153), H2 (residues 172−192), and H3 (residues 200−225), as well as a small antiparallel β-sheet composed of two β-strands, namely, S1 (residues 129 and 130) and S2 (residues 162 and 163). Its function is not fully understood, but it putatively contributes to transport of copper, neuronal morphology, adhesion, and regulation of lymphocytes.[5,6]

The past decades have seen the extension of our knowledge of prion proteins with the solution of NMR and X-ray structures of various species[7−10] culminating in the elucidation of human prion proteins.[11−13] Important advances in relating disease to structure have also been made through the identification of the minimal prion protein fragment that is capable of conferring propagation of the scrapie agent.[3] Despite these studies, the transition from PrP^C to PrP^{Sc} remains poorly understood, and structures of the monomeric isoforms and oligomers are still unresolved. Fourier-transform infrared (FTIR) spectroscopy and circular dichroism (CD) showed a substantial difference in the secondary structure content of PrP^C and PrP^{Sc}. PrP^C displayed high α-helix content (42%) and little or no β-sheet content (3%), while PrP^{Sc} showed a high β-sheet content (43%) and a less pronounced α-helix content (30%).[6] These findings suggest that the conversion of α-helices into β-sheets is a fundamental event in the formation of PrP^{Sc} and propagation of prion diseases.

Normal-mode analysis is one of the standard techniques for studying long-time dynamics and, in particular, low-frequency motions. In contrast to molecular dynamics, normal-mode analysis provides a very detailed description of the dynamics around a local energy minimum. Even with its limitations, such as the neglect of the solvent effect, the use of harmonic approximation of the potential energy function, and the lack of information about energy barriers and crossing events, normal modes have provided much useful insight into protein dynamics. Over the past several years, several techniques for calculating large-scale motions using classical[14−16] and simplified[17−20] normal-mode analysis have been described. On the basis of these techniques, several executable programs for calculating normal modes have been released, such as ElNemo,[21] Nomad-ref,[22] and Normod (unpublished). Similarly, molecular dynamics programs such as GROMACS[23] were modulated to calculate normal modes. Using these programs, several molecular dynamics studies have been conducted.

A large number of studies using elastic network models to analyze the molecular dynamics and activity of biological molecules have been conducted (reviewed in refs[24−26]). In this study,

Received: July 1, 2010
Revised: February 11, 2011
Published: February 21, 2011

Table 1. Consensus Secondary Structure of Prion Protein (PDB entry 3HAK) in the Native and Normal-Mode Distorted Structures

```
                .         .         .         .         .
SEQ 125   LGGYVLGSAMSRPIIHFGSDYEDRYYRENMHRYPNQVYYRPMDEYSNQNN  174
Native        EE             HHHHHHHHHHGGG     EE GGGGG  HHH
Distorted     EEEEE            HHHHHHHHGGG  EEEEE GGGGG  HHH

                .         .         .         .         .
SEQ 175   FVHDCVNITIKQHTVTTTTKGENFTETDVKMMERVVEQMCITQYERESQA  224
Native    HHHHHHHHHHHHHHHHHHH      HHHHHHHHHHHHHHHHHHHHHHHHH
Distorted HHHHHHHHHHHHHHHHHHH      HHHHHHHHHHHHHHHHHHHHHHHHH
```

we calculate the normal modes of various prion proteins and assess the conformational transition between PrP^C and PrP^{Sc}. To the best of our knowledge, this is the first attempt to characterize the conformational change of prion proteins using normal modes. We find that normal modes display an increase in β-sheet content alongside a reduction in α-helical content. These findings broaden our understanding of the conformational transition associated with prion protein infection.

COMPUTATIONAL PROCEDURES

Normal-Mode Calculations. To calculate normal modes of the prion proteins, two programs, Normod[16] and ElNemo,[21] were utilized. The normal-mode calculations were run locally on a Linux (Ubuntu 8.04) operated desktop computer with a 1.8 GHz Intel Pentium processor and 2 GB of RAM. For Normod, normal modes based on realistic force fields (REA) and on elastic network models (TIR) were calculated. For ElNemo, the following default values were utilized: DQMIN, −100; DQMAX, 100; DQSTEP, 20. For both Normod and ElNemo, the 10 nontrivial lowest-frequency modes were calculated. For each of these 10 lowest-frequency modes, ensembles of 40 Protein Data Bank (PDB) files were generated by Normod and 10 PDB files by ElNemo all distorted along the particular mode. The two methods are very different in that Normod (REA) minimizes the structure and then calculates modes in single-bond torsion angle space whereas Normod (TIR) and ElNemo avoid minimization by using Tirion elastic motion[17] and a coarse-grained elastic network model,[18,19] respectively, and then calculate modes in Cartesian coordinate space. Normal modes of the following prion protein PDB entries were calculated: 3HAK, 3HAF, 3HEQ, 3HER, and 3HES. If the PDB structures contained a dimer, only one monomer was used.

Secondary Structure Calculation. To calculate the secondary structure of native structures as well as those distorted along normal modes, we utilized several programs. The use of several programs was necessary as not all programs calculate identical secondary structure. The programs that were utilized were Stride,[27] DSSP,[28] and Encad.[29] The consensus secondary structure was considered as that calculated by two of three programs.

Secondary Structure Probability. To calculate the secondary structure probability of prion proteins, we used NetSurfP described by Petersen et al.[30]

Modeling of the PrP^C Isoform and PrP^{Sc}. To construct a model of the PrP^C isoform, the β-sheet of PDB entry 3HAK was elongated to comprise residues 129−163 (S1, S2, and H1). To construct the two models of PrP^{Sc}, the trimeric model postulated by Govaerts et al.[31] was used as a template. The first model is a trimer of the PrP^C isoforms in which the β-sheets are stacked so they can form parallel intermolecular β-sheets. The second model is a trimer of the PrP^C isoforms in which the N-terminus was replaced with a β-helical conformation modeled by Govaerts et al. All models were prepared using Pymol.

RESULTS AND DISCUSSION

Normal Modes of Prion Proteins. The normal modes of several prion proteins (PDB entries 3HAK, 3HAF, 3HEQ, 3HER, and 3HES) were calculated. Remarkably, the lowest-frequency mode of PDB entries 3HAK, 3HAF, and 3HER exhibited an increase in β-structure content and a decrease in α-structure content (Table 1). Other modes also displayed this change; however, most often, the first one or two normal modes are enough to describe molecular motions,[32] and we decided to focus on the lowest-frequency mode.

The conformational change calculated by normal modes corresponds to a 6% increase in β-sheet structure content and a 3% decrease in α-helix content. This conformational change is very small and less pronounced than that observed experimentally,[6] and hence, the small increase in β-sheet content and the decrease in α-helix content should be regarded more like a qualitative tendency. We do not claim to have detected a secondary structure change from α-helix to β-sheet (i.e., α-helix turned into β-sheet). We claim that there is an overall increase in β-structure content and a decrease in α-helical content (i.e., random coil changed into β-structure and α-structure changed into random coil).

The region undergoing the conformational change is consistent with experimental data. Immunological experiments indicated that the major conformational changes that differentiate PrP^C and PrP^{Sc} take place in the N-terminal region,[33] because two antibodies targeting the C-terminal helices of PrP^C also recognize PrP^{Sc}. The conformational preservation of these α-helices is also supported by the existence of a disulfide bridge that conjoins them. Therefore, in PrP^C, the main conformational change that occurs in the N-terminal region between residues 89 and 172 is in agreement with the region predicted by normal-mode dynamics.

The square displacement of Cα atoms in the prion proteins that is associated with the lowest-frequency mode is shown in Figure 1. The Cα square displacement values of different prion structures were scaled to fit in the same graph. Large Cα displacements occur in segments with disordered secondary structure, while the low level of motion is observed in secondary structure elements. Nevertheless, the displacement around H1 is sufficiently large to disrupt hydrogen bonds and partially unwind

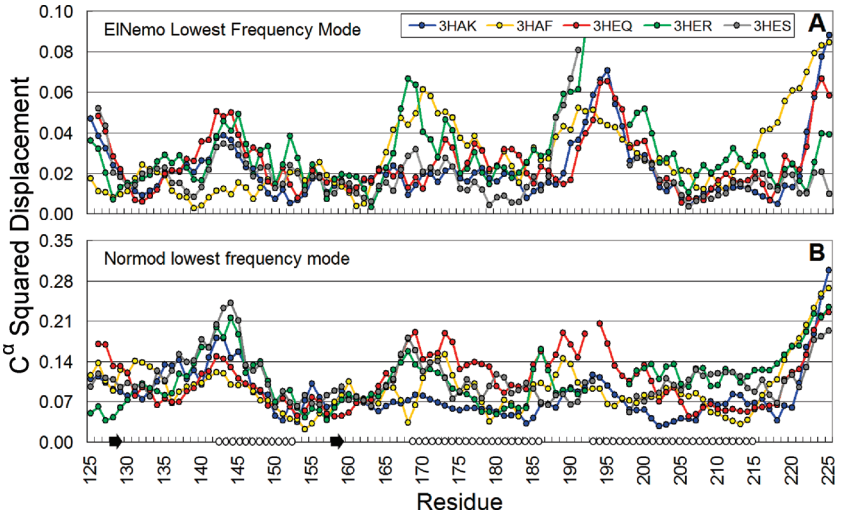

Figure 1. Scaled square displacement of Cα atoms of prion proteins. Shown are the scaled Cα square displacement values of the (A) ElNemo and (B) Normod lowest-frequency mode of PDB entries 3HAK, 3HAF, 3HEQ, 3HER, and 3HES. The secondary structure is indicated above the residue axis. Note the minimal displacement around helices and sheets.

this α-helix. The displacement around β-strands S1 and S2 allows the elongation of the antiparallel β-sheet.

Prion Protein Dynamics. A superposition of the ensemble of structures of the lowest-frequency mode that were generated using ElNemo is shown in Figure 2. During this mode, the opposite β-strands S1 and S2 come close, thereby forming new hydrogen bonds that allow the extension of the β-sheet. This increase in β-sheet content is in agreement with experimental data.[6]

Normal modes provide a very detailed description of the long-term dynamics around a local energy minimum. As such, these data provide reasonable insight into how spontaneous occurrences of TSE might begin (not end). The conformational transition from the α-helical to the β-rich isoform is separated by a large energetic barrier, yet transformation to the prion form seems to occur spontaneously at 10^{-6}–10^{-7} frequencies during mis- and refolding of yeast proteins.[34] For the spontaneous occurrence of TSE, spontaneous conversion similar to that instigated during normal modes and involving the β-sheet elongation mechanism is proposed. For transmitted TSE, propagation of prion forms is triggered by interaction of the normal PrP^{C} with mutant PrP^{Sc}, though it is not clear yet whether the PrP^{Sc} oligomer acts as a seed or the PrP^{Sc} monomer acts as a template for conformational change.[34] In any case, the large energetic barrier between the α-helical and β-rich isoforms is lowered and conversions between these two states become more frequent. For both spontaneous and transmitted TSE, the conversion is initiated by zipping together β-strands S1 and S2. Such "zipping" mechanisms are common in protein structural conversions and were postulated for polar zippers by Max Perutz[35] and steric zippers of amyloid-like fibrils.[36]

In vivo, prion proteins are glycosylated on residues N181 and N197. These sugar moieties contribute to the stability of the PrP by sterically occluding denaturing interactions[37] without which it would be more prone to conversion. Interestingly, if the sugar moieties were included in the normal-mode calculation of the prion protein, then the lowest-frequency normal modes showed only bending of the sugar masses and displayed no secondary structure changes (data not shown). This finding is in line with the protective role of the carbohydrates observed experimentally. Finally, the long N-terminus of the PrP was not included as there is no structure available at this time.

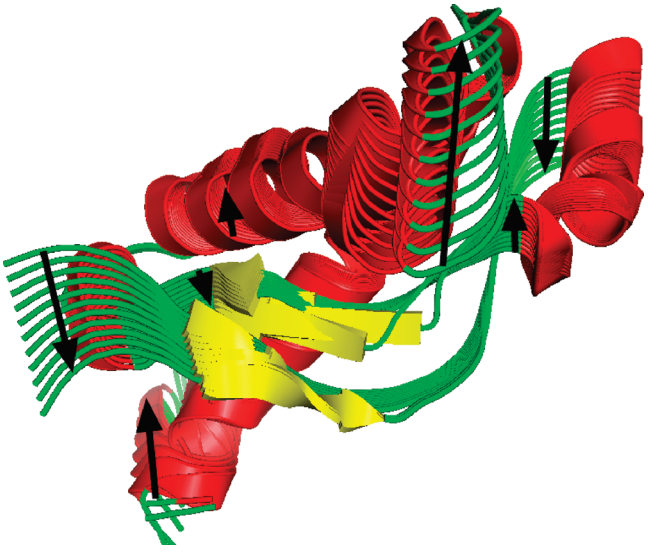

Figure 2. Lowest-frequency mode of prion proteins. Shown in cartoon display are the ensemble structures of the lowest-frequency mode of ElNemo of PDB entry 3HAK. Arrows denote the directions of simultaneous motion in time. Note the elongation of β-strands S1 and S2 (yellow) that leads to the lengthening of the antiparallel β-sheet.

Previous studies of amyloid fibrils using elastic network modeling studies were reported and showed bending and tensile deformation of the fibrils.[38] Also, amyloid nanofibrils exhibit elasticities varying by 4 orders of magnitude depending on the amino acid sequence.[39] These studies on amyloid fibrils, however, did not have the same intention as our work; to the best of our knowledge, this is the first attempt to characterize prion protein conformational changes using normal modes.

Propensity for β-Structure. Shown in Figure 3 is the secondary structure probability for the human prion protein as well

dx.doi.org/10.1021/bi1010514 |*Biochemistry* 2011, 50, 2243–2248

as the actual secondary structure of PDB entry 3HAK. The correlation between the β-strand probability and the actual β-sheet content is almost perfect. The regions between the secondary structure elements, in random loop conformation, also correspond to the experimental data. The correlation between helical regions and actual α-helices is a bit less obvious. This could indicate an easy transition from α-helix to β-strand conformation in the latter region.

Interestingly, elastic network modes of the mutant V129 prions (PDB entries 3HAK, 3HAF, and 3HER) exhibited β-sheet elongation of S1 and S2, while native M129 prions (PDB entries 3HEQ and 3HES) did not (data not shown). Because the motion exhibited by M129 and V129 prions is very similar (Figure 1), the diverging final secondary structures are mainly attributed to differences in the starting structures that are amplified through the normal-mode motion. For example, the distance between the Cα atoms of residues S132 and Q160 that elongate the β-sheet is shorter in the V129 prion (4.5 Å in PDB entry 3HAK) than in the M129 prion (6.0 Å in PDB entry 3HES). The common methionine/valine polymorphism at residue 129 is a factor that influences prion disease susceptibility. Lee et al.[13] suggested that the disease susceptibility of V129 stems from the inclination of prion proteins to dimerize as seen in crystals of prion proteins containing V129, which revealed both dimeric and monomeric structures. We think that V129 plays an additional role in disease susceptibility as valine has a stronger propensity for β-structure than methionine.[40] V129 is located in the center of the first strand (S1) and thus stabilizes the antiparallel β-sheet. The stronger propensity for β-sheet, which increases the risk of conversion to PrP^{Sc}, works in synergy with the dimerization susceptibility, by lowering the energy barrier to formation of PrP^{Sc}.

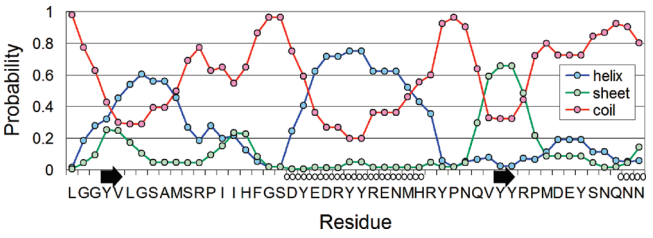

Figure 3. Secondary structure probability of the human M129V mutant prion protein. Shown is the probability for helix, sheet, and coil formation of the M129V mutant prion protein (residues 125−174) calculated using NetSurfP.[30] The actual secondary structure of PDB entry 3HAK is indicated above the residue axis.

Structure of PrP^{Sc}. To date, there is no published structure of PrP^{Sc}. The absence of such a structure has made it quite challenging to assess the exact pathway of conversion between PrP^{C} and PrP^{Sc}. One study suggested that if PrP^{Sc} followed a known protein fold, it would adopt either a parallel β-helical or a β-sandwich architecture in a trimeric assembly[31] (Figure 4). Our

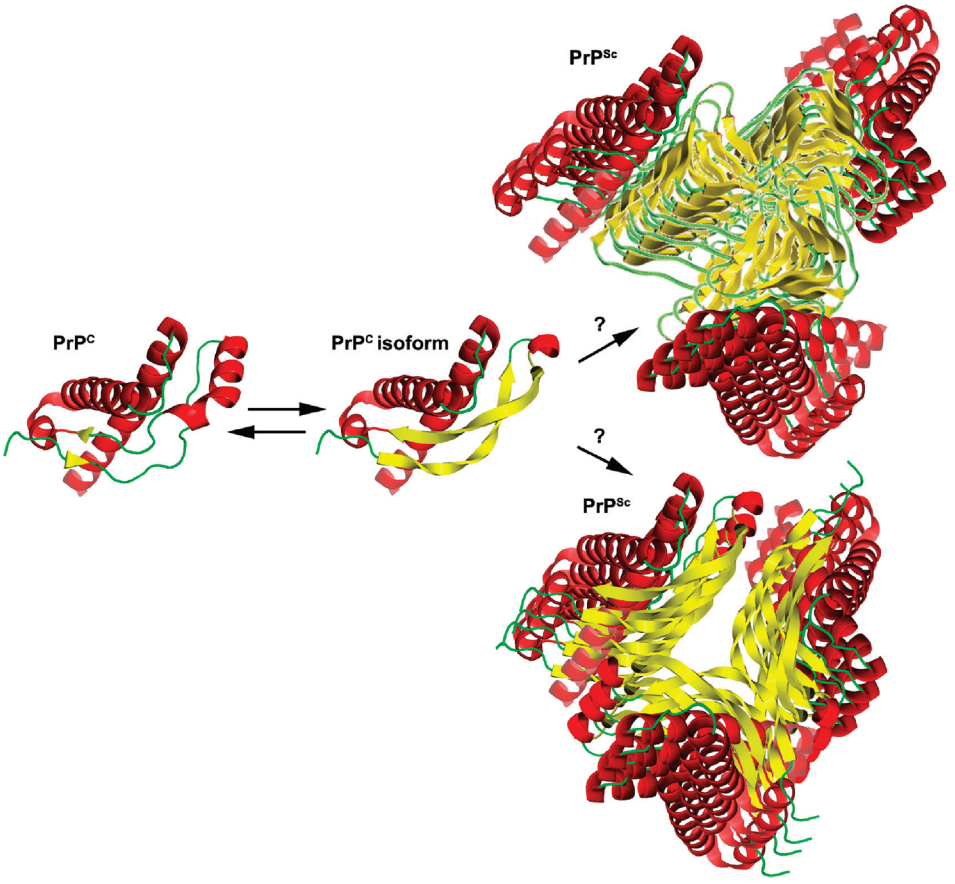

Figure 4. Model of the PrP^{C} isoform and PrP^{Sc}. Shown are cartoon representations of the PrP^{C} structure, putative PrP^{C} isoform, and two PrP^{Sc} models. PrP^{C} corresponds to PDB entry 3HAK. The PrP^{C} isoform is similar to PrP^{C} with the exception of a β-sheet elongation. PrP^{Sc} models were based on the trimeric assembly reported by Govaerts et al.[31] In the top PrP^{Sc}, the N-terminus adopts a β-helix conformation. In the bottom PrP^{Sc}, the N-terminus adopts a β-sandwich conformation similar to the steric zipper conformation reported by Nelson et al.[36] This figure was prepared using Pymol.

normal-mode calculations indicate an elongation of the antiparallel β-sheet into a β-hairpin, which supports the latter opinion, but both are admissible (Figure 4). The β-sandwich could form upon stacking (dimerization) of one β-hairpin of PrP^{Sc} onto another, in line with the idea of steric zippers.[36] In Figure 4, the lower PrP^{Sc} model oligomerizes by steric stacking of elongated β-sheets (β-sandwich-like). Several β-sandwich architectures are available from the SCOP database,[41] and without further experimental data, it is hard to predict the exact PrP^{Sc} structure. Alternatively, the parallel β-helical or β-sandwich architecture could form upon PrP^{C} dimerization followed by a domain swap mechanism.[42] The swap mechanism involves exchange of domains between two proteins (not shown). This working hypothesis is reinforced by the fact that several studies have observed PrP^{C} dimerization to have an important role in the formation of PrP^{Sc}.[13] Prion proteins consist of two main domains: (1) S1, H1, and S2 and (2) H2 and H3. In the lowest-frequency mode, these two domains move independently as they have only a few interactions (see the Supporting Information). The independence of the two domains is what allows domains to be swapped more readily. These normal-mode data improve our understanding of amyloid formation in TSE of prions.

CONCLUSION

The mechanism of conformational change that instigates PrP infection was evaluated through normal modes. The normal modes display a decrease in the α-helical content along with an increase in the β-structure content both occurring in the region involved in PrP conversion through a zipper mechanism. These findings are valuable for our comprehension of the conversion mechanism associated with the conformational change of prion proteins.

ASSOCIATED CONTENT

Supporting Information. Movies of the normal-mode vibration of PrP^{C} (PDB entry 3HAK). This material is available free of charge via the Internet at http://pubs.acs.org.

AUTHOR INFORMATION

Corresponding Author

*Department of Structural Biology, Stanford University, Stanford, CA 94305. Telephone: (650) 725-0754. Fax: (650) 723-8464. E-mail: avraham.samson@stanford.edu.

Funding Sources

This research was supported by National Institutes of Health (NIH) Roadmap for Medical Research Grant PN2 EY016525 and NIH Grant GM41455.

ACKNOWLEDGMENT

We thank Dr. Dahlia Weiss for careful reading of the manuscript.

ABBREVIATIONS

TSE, transmissible spongiform encephalopathies; PrP, prion protein; PrP^{C}, cellular form of PrP; PrP^{Sc}, scrapie form of PrP.

REFERENCES

(1) Prusiner, S. B. (1982) Novel proteinaceous infectious particles cause scrapie. *Science 216*, 136–144.

(2) Prusiner, S. B., McKinley, M. P., Bowman, K. A., Bolton, D. C., Bendheim, P. E., Groth, D. F., and Glenner, G. G. (1983) Scrapie prions aggregate to form amyloid-like birefringent rods. *Cell 35*, 349–358.

(3) Jackson, G. S., and Clarke, A. R. (2000) Mammalian prion proteins. *Curr. Opin. Struct. Biol. 10*, 69–74.

(4) Belay, E. D. (1999) Transmissible spongiform encephalopathies in humans. *Annu. Rev. Microbiol. 53*, 283–314.

(5) Isaacs, J. D., Jackson, G. S., and Altmann, D. M. (2006) The role of the cellular prion protein in the immune system. *Clin. Exp. Immunol. 146*, 1–8.

(6) Pan, K. M., Baldwin, M., Nguyen, J., Gasset, M., Serban, A., Groth, D., Mehlhorn, I., Huang, Z., Fletterick, R. J., and Cohen, F. E. (1993) Conversion of α-helices into β-sheets features in the formation of the scrapie prion proteins. *Proc. Natl. Acad. Sci. U.S.A. 90*, 10962–10966.

(7) Liu, H., Farr-Jones, S., Ulyanov, N. B., Llinas, M., Marqusee, S., Groth, D., Cohen, F. E., Prusiner, S. B., and James, T. L. (1999) Solution structure of Syrian hamster prion protein rPrP(90−231). *Biochemistry 38*, 5362–5377.

(8) James, T. L., Liu, H., Ulyanov, N. B., Farr-Jones, S., Zhang, H., Donne, D. G., Kaneko, K., Groth, D., Mehlhorn, I., Prusiner, S. B., and Cohen, F. E. (1997) Solution structure of a 142-residue recombinant prion protein corresponding to the infectious fragment of the scrapie isoform. *Proc. Natl. Acad. Sci. U.S.A. 94*, 10086–10091.

(9) Liu, H., Spielmann, H. P., Ulyanov, N. B., Wemmer, D. E., and James, T. L. (1995) Interproton distance bounds from 2D NOE intensities: Effect of experimental noise and peak integration errors. *J. Biomol. NMR 6*, 390–402.

(10) Calzolai, L., Lysek, D. A., Perez, D. R., Guntert, P., and Wuthrich, K. (2005) Prion protein NMR structures of chickens, turtles, and frogs. *Proc. Natl. Acad. Sci. U.S.A. 102*, 651–655.

(11) Calzolai, L., Lysek, D. A., Guntert, P., von Schroetter, C., Riek, R., Zahn, R., and Wuthrich, K. (2000) NMR structures of three single-residue variants of the human prion protein. *Proc. Natl. Acad. Sci. U.S.A. 97*, 8340–8345.

(12) Zahn, R., Liu, A., Luhrs, T., Riek, R., von Schroetter, C., Lopez Garcia, F., Billeter, M., Calzolai, L., Wider, G., and Wuthrich, K. (2000) NMR solution structure of the human prion protein. *Proc. Natl. Acad. Sci. U.S.A. 97*, 145–150.

(13) Lee, S., Antony, L., Hartmann, R., Knaus, K. J., Surewicz, K., Surewicz, W. K., and Yee, V. C. (2010) Conformational diversity in prion protein variants influences intermolecular β-sheet formation. *EMBO J. 29*, 251–262.

(14) Brooks, B., and Karplus, M. (1983) Harmonic dynamics of proteins: Normal modes and fluctuations in bovine pancreatic trypsin inhibitor. *Proc. Natl. Acad. Sci. U.S.A. 80*, 6571–6575.

(15) Go, N., Noguti, T., and Nishikawa, T. (1983) Dynamics of a small globular protein in terms of low-frequency vibrational modes. *Proc. Natl. Acad. Sci. U.S.A. 80*, 3696–3700.

(16) Levitt, M., Sander, C., and Stern, P. S. (1985) Protein normal-mode dynamics: Trypsin inhibitor, crambin, ribonuclease and lysozyme. *J. Mol. Biol. 181*, 423–447.

(17) Tirion, M. M. (1996) Large Amplitude Elastic Motions in Proteins from a Single-Parameter, Atomic Analysis. *Phys. Rev. Lett. 77*, 1905–1908.

(18) Atilgan, A. R., Durell, S. R., Jernigan, R. L., Demirel, M. C., Keskin, O., and Bahar, I. (2001) Anisotropy of fluctuation dynamics of proteins with an elastic network model. *Biophys. J. 80*, 505–515.

(19) Tama, F., and Sanejouand, Y. H. (2001) Conformational change of proteins arising from normal mode calculations. *Protein Eng. 14*, 1–6.

(20) Delarue, M., and Sanejouand, Y. H. (2002) Simplified normal mode analysis of conformational transitions in DNA-dependent polymerases: The elastic network model. *J. Mol. Biol. 320*, 1011–1024.

(21) Suhre, K., and Sanejouand, Y. H. (2004) ElNemo: A normal mode web server for protein movement analysis and the generation of templates for molecular replacement. *Nucleic Acids Res. 32*, W610–W614.

(22) Lindahl, E., Azuara, C., Koehl, P., and Delarue, M. (2006) NOMAD-Ref: Visualization, deformation and refinement of macromolecular structures based on all-atom normal mode analysis. *Nucleic Acids Res. 34*, W52–W56.

(23) Van Der Spoel, D., Lindahl, E., Hess, B., Groenhof, G., Mark, A. E., and Berendsen, H. J. (2005) GROMACS: Fast, flexible, and free. *J. Comput. Chem. 26*, 1701–1718.

(24) Taly, A., Corringer, P. J., Grutter, T., Prado de Carvalho, L., Karplus, M., and Changeux, J. P. (2006) Implications of the quaternary twist allosteric model for the physiology and pathology of nicotinic acetylcholine receptors. *Proc. Natl. Acad. Sci. U.S.A. 103*, 16965–16970.

(25) Samson, A. O., and Levitt, M. (2008) Inhibition mechanism of the acetylcholine receptor by α-neurotoxins as revealed by normal-mode dynamics. *Biochemistry 47*, 4065–4070.

(26) Bahar, I., Lezon, T. R., Yang, L. W., and Eyal, E. (2010) Global dynamics of proteins: Bridging between structure and function. *Annu. Rev. Biophys. 39*, 23–42.

(27) Frishman, D., and Argos, P. (1995) Knowledge-based protein secondary structure assignment. *Proteins 23*, 566–579.

(28) Kabsch, W., and Sander, C. (1983) Dictionary of protein secondary structure: Pattern recognition of hydrogen-bonded and geometrical features. *Biopolymers 22*, 2577–2637.

(29) Levitt, M. (1983) Molecular dynamics of native protein. I. Computer simulation of trajectories. *J. Mol. Biol. 168*, 595–617.

(30) Petersen, B., Petersen, T. N., Andersen, P., Nielsen, M., and Lundegaard, C. (2009) A generic method for assignment of reliability scores applied to solvent accessibility predictions. *BMC Struct. Biol. 9*, 51.

(31) Govaerts, C., Wille, H., Prusiner, S. B., and Cohen, F. E. (2004) Evidence for assembly of prions with left-handed β-helices into trimers. *Proc. Natl. Acad. Sci. U.S.A. 101*, 8342–8347.

(32) Krebs, W. G., Alexandrov, V., Wilson, C. A., Echols, N., Yu, H., and Gerstein, M. (2002) Normal mode analysis of macromolecular motions in a database framework: Developing mode concentration as a useful classifying statistic. *Proteins 48*, 682–695.

(33) Peretz, D., Williamson, R. A., Matsunaga, Y., Serban, H., Pinilla, C., Bastidas, R. B., Rozenshteyn, R., James, T. L., Houghten, R. A., Cohen, F. E., Prusiner, S. B., and Burton, D. R. (1997) A conformational transition at the N terminus of the prion protein features in formation of the scrapie isoform. *J. Mol. Biol. 273*, 614–622.

(34) Tuite, M. F., and Cox, B. S. (2003) Propagation of yeast prions. *Nat. Rev. Mol. Cell Biol. 4*, 878–890.

(35) Perutz, M. F. (1995) Glutamine repeats as polar zippers: Their role in inherited neurodegenerative disease. *Mol. Med. 1*, 718–721.

(36) Nelson, R., Sawaya, M. R., Balbirnie, M., Madsen, A. O., Riekel, C., Grothe, R., and Eisenberg, D. (2005) Structure of the cross-β spine of amyloid-like fibrils. *Nature 435*, 773–778.

(37) Rudd, P. M., Wormald, M. R., Wing, D. R., Prusiner, S. B., and Dwek, R. A. (2001) Prion glycoprotein: Structure, dynamics, and roles for the sugars. *Biochemistry 40*, 3759–3766.

(38) Xu, Z., Paparcone, R., and Buehler, M. J. (2010) Alzheimer's Aβ(1−40) amyloid fibrils feature size-dependent mechanical properties. *Biophys. J. 98*, 2053–2062.

(39) Knowles, T. P., Fitzpatrick, A. W., Meehan, S., Mott, H. R., Vendruscolo, M., Dobson, C. M., and Welland, M. E. (2007) Role of intermolecular forces in defining material properties of protein nanofibrils. *Science 318*, 1900–1903.

(40) Chou, P. Y., and Fasman, G. D. (1974) Conformational parameters for amino acids in helical, β-sheet, and random coil regions calculated from proteins. *Biochemistry 13*, 211–222.

(41) Murzin, A. G., Brenner, S. E., Hubbard, T., and Chothia, C. (1995) SCOP: A structural classification of proteins database for the investigation of sequences and structures. *J. Mol. Biol. 247*, 536–540.

(42) Staniforth, R. A., Giannini, S., Higgins, L. D., Conroy, M. J., Hounslow, A. M., Jerala, R., Craven, C. J., and Waltho, J. P. (2001) Three-dimensional domain swapping in the folded and molten-globule states of cystatins, an amyloid-forming structural superfamily. *EMBO J. 20*, 4774–4781.